https://doi.org/10.48048/tis.2023.5339

Effects of Crescent Shaped Block Width and Length on Flow Field and Film Cooling Performance

Guelailia Ahmed[1,2,*], Khorsi Azzeddine[2], Slimane Sid Ahmed[1,2], Blala Hamza[1] and Slimane Abdelkader[2,3]

[1]Space Mechanical Research Department, Centre of Satellite Development, Algerian Space Agency, Oran, Algeria
[2]Laboratory of Applied Mechanics, Faculty of Mechanical Engineering, University of Sciences and Technology Mohamed Boudiaf, Oran, Algeria
[3]Laboratory of Materials and Reactive Systems, Department of Mechanical Engineering, University Djilali Liabes, Sidi Bel Abbes, Algeria

([*]Corresponding author's e-mail: guelailia@yahoo.fr)

Received: 21 July 2022, Revised: 5 September 2022, Accepted: 12 September 2022, Published: 17 March 2023

Abstract

Turbine blades and rocket nozzles can be efficiently protected from combustion chamber exhaust hot gases by film cooling technic. A crescent-shaped block placed downstream of the injection hole can significantly improve cooling effectiveness. The main objective of this research work is to investigate the influence of the crescent-shaped block length and width on film cooling effectiveness. ANSYS CFX was used to conduct analysis of a flat plate configuration with cylindrical holes. Nine configurations of the crescent shaped blocks were considered. For each case, the effect of blowing ratios (0.5 and 1) was investigated. The turbulence model shear stress transport (SST) is used for approximating turbulence. Good agreement was obtained by comparing the analysis results with the experimental data. The result indicated that block width variation has a considerable impact on film cooling performance. However, slight effect of block length on cooling effectiveness was obtained. Comparing all analyzed configurations, the best cooling effectiveness was reached for the model 9 (W = 3d, B = 1.5d).

Keywords: Blowing ratio, Computational fluid dynamics, Film cooling, Thermal protection

Introduction

Optimizing the efficiency of thermal engines like gas turbines, rockets and turbojets is a very important challenge that engineers and researchers are interested in. Increasing the temperature of combustion chambers can improve the performance of such engines. However, the heat emitted from the combustion chamber exceeds the material failure limits of the thermal engine components. We must thus ensure an efficient thermal protection system of the hot components such as turbine blade walls and rocket nozzles. Film cooling method was frequently employed for protecting engine component walls from hot gases of combustion chamber. In this cooling process, the coolant is pumped on the component walls through holes. A thin layer of thermal insulation is formed on the surface due to the interaction of the mainstream hot flow and the cold flow, which prevents the wall to be damaged by the superheated flow.

In recent years, considerable effort was devoted to improve cooling performance which is affected by many physical and geometrical parameters. The physical properties such as: ratio of temperature, density, pressure of the 2 flows, blowing ratio and turbulence intensity have a significant effect on film cooling. Ammari and Lampard [1] carried out a research study to analyze the density impact on film cooling. The findings showed that changing the density ratio affects significantly the heat transfer coefficient, particularly for 35 ° of injection angle. The influence of density ratio and blowing ratio on film cooling effectiveness was experimentally investigated by Sinha *et al.* [2]. It was indicated that the laterally averaged effectiveness is strongly related on blowing ratio and density. Drost and Bölcs [3] experimentally investigated the heat transfer thought a blade of gas turbine. Experiments has been performed at different mainstream turbulence intensities and different Reynolds numbers. The results show that the coolant structure on suction side is affected by the variations in Reynolds and Mach number.

Also, enhancing the injection holes' shape; their location and distribution can highly optimize the film cooling performance. Film cooling experiments on the leading edge of a turbine blade were conducted by Liu *et al.* [4]. Two shapes of perforation are tested: converged slots and cylindrical perforations. Guelailia

et al. [5] conducted a numerical investigation to study the mass flow rate effect on heat transfer over a rotor blade of gas turbine. To improve film cooling performance, the converging slot holes are used instead of the cylindrical holes. The results indicated that the new hole shape (consol) provides better thermal protection than ordinary cylindrical perforations. Several configurations of film cooling holes such as: fan-shaped hole, combined hole and conical hole were tested in the research study of Wang *et al.* [6]. More uniform cooling film was obtained by the combined hole configuration compared to the fan-shaped and conical holes. Cao *et al*. [7] investigated experimentally and numerically the effect of perforation geometry on coolant structure. The influence of hole blockage on film cooling performance was analyzed by Tian *et al.* [8]. Schmidt and Bogard [9], Schmidt *et al.* [10]., Goldstein *et al.* [11] investigated the impact of wall roughness on film cooling characteristics, they noticed a slight degradation in cooling performance. A numerical study was conducted by Guelailia *et al.* [12] to investigate the effects of depositions position and height on cooling efficiency. Yuen and Martinez-Botas [13,14] provided in their research papers results of heat transfer for a flat plate configuration. In order to enhance film cooling effectiveness, new hole shape of film cooling (lidded hole) was proposed in the work of Guelailia *et al.* [15]. The effects of surface radial and longitudinal curvature on the performance of film cooling was investigated by Guelailia *et al.* [16,17]. Kumar *et al.* [18] investigated the influence of cold flow injector of a rocket nozzle divergent section on film cooling effectiveness.

One of the latest techniques to optimize the overall performance of film cooling is adding an obstacle configuration downstream the coolant perforation. Results presented in the work of Khorsi *et al.* [19] indicated that the block shaped as a crescent promises significant enhancement of cooling effectiveness. Recently, the effect of longitudinal curvature on film cooling performance was analyzed by Guelailia *et al.* [20]. The goal of this work is to study the influence the crescent block length and width on film cooling characteristics at several blowing ratios by using ANSYS CFX code. The results obtained are compared to the results obtained experimentally by Nasir *et al.* [21]. The following questions are addressed in this research paper:

1) How can the crescent block improve the performance of film cooling and what is the effects of block width (W) and length (B) on the coolant distribution and flow structure?

2) How can blowing ratio impact the efficiency of lateral and centerline film cooling of crescent shaped block cases?

To answer such concerns, the problem is numerically studied by conducting 3D numerical simulations using ANSYS CFX commercial software code.

Numerical method

In the present study, the CFD software ANSYS CFX was used to conduct the 3-dimensional simulations. In the solver module, the equations of continuity (1), momentum (2), and energy (3) was discretized using the method of finite volume.

$$\frac{\partial \rho}{\partial t} + \nabla \bullet \left(\rho U \right) = 0 \tag{1}$$

$$\frac{\partial (\rho U)}{\partial t} + \nabla \bullet (\rho U \otimes U) = \nabla \bullet \left(- p\delta + \tau - \rho \overline{u \otimes u} \right) + S_M \tag{2}$$

$$\frac{\partial (\rho h_{tot})}{\partial t} - \frac{\partial p}{\partial t} + \nabla \bullet (\rho U h_{tot}) = \nabla \bullet (\lambda \nabla T) + \nabla \bullet (U\tau) + U \bullet S_M + S_E \tag{3}$$

where $h_{tot} = h + \frac{1}{2}U^2$ (4)

The SST (shear stress transport) model of Menter *et al.* [22] approximates turbulence. The numerical simulation is performed until achieving the convergence condition (10^{-5}).

Geometry

The computation domain geometry with the crescent shaped block is presented in **Figure 1**. The length of film cooling injection cylindrical holes is L/d = 6 and the diameter is d = 12.7 mm. The computation domain dimensions are 45d*5d*3d by coordinates x, y, z. The film cooling hole is inclined

with a 35 ° of streamwise angle. The plane of exit is fixed at x/d = 30 downstream from the injection hole centre, while the inlet is at x/d = 15 upstream. The height of the calculation domain is y/d = 5. The used block is characterised by the several geometrical parameters: δ, W, B, λ and H as illustrated in **Figure 1**. Note that only the height of the block is kept constant H/d = 0.25. Nine configurations were tested by changing the width and length of the crescent block. **Figure 2** illustrates the geometries considered. The geometrical characteristics of all investigated models are shown in the **Table 1**.

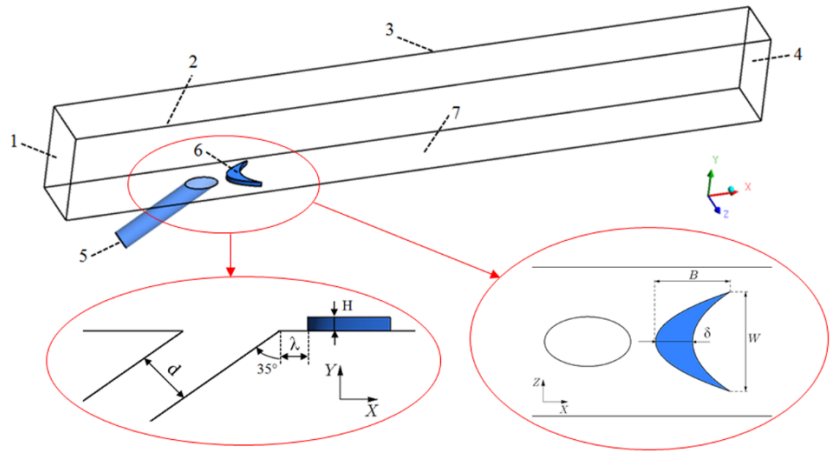

Figure 1 Geometry of the configuration: 1) hot flow inlet, 2) plane of symmetry 1, 3) plane of symmetry 2, 4) outlet, 5) cold flow inlet, 6) Crescent shaped block and 7) cooled surface.

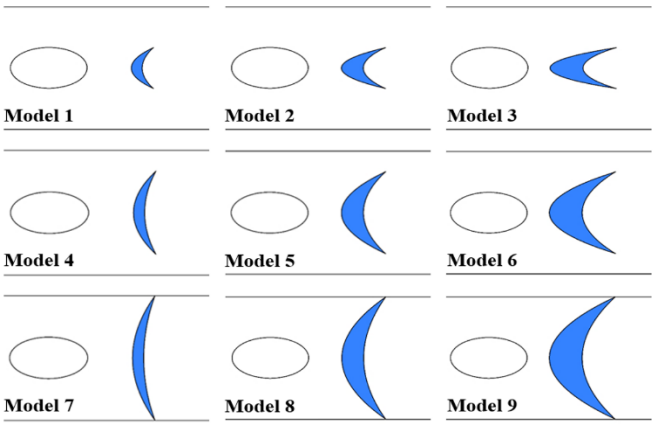

Figure 2 Geometries of various crescent-shaped blocks.

Table 1 Geometrical parameters of different crescent shaped block cases.

Model	W/d	B/d	δ/d	λ/d
Model 1	1	0.5	0.25	1
Model 2	1	1	0.5	0.75
Model 3	1	1.5	0.75	0.5
Model 4	2	0.5	0.25	1
Model 5	2	1	0.5	0.75
Model 6	2	1.5	0.75	0.5
Model 7	3	0.5	0.25	1
Model 8	3	1	0.5	0.75
Model 9	3	1.5	0.75	0.5

Mesh generation

The commercial mesh software ICEM CFD was employed to generate the computational grid. A structured multi-block mesh is used to discretize the computation domain. Three different structured grids were created and named: coarse, medium, and fine. The baseline configuration was used to perform a grid independence study. The maximum change percent between moderate and coarse meshes is 25 %. However, no difference was observed between moderate and fine meshes. The moderate mesh which consists of 1032404 hexahedral elements was chosen in the present paper. The grid was refined near the walls and especially near the crescent shaped block and the injection hole areas. At near-wall nodes, the values of y^+ was kept within the requirements of the turbulence model used SST ($y^+ < 2$). **Figure 3** presents the structured multi-block mesh used for this CFD numerical analysis.

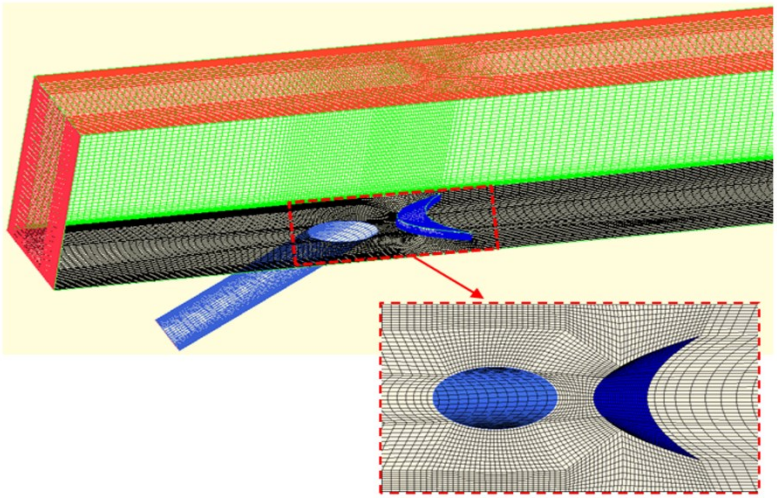

Figure 3 Computational grid.

Boundary conditions

The physical parameters and the boundary condition details are presented in the **Table 2**. no-slip adiabatic walls conditions were imposed for the cooled surface, upper domain and perforation walls. The two lateral planes were assigned to be symmetry conditions. The hot flow temperature $T_\infty = 331.15$ K, cold jet temperature $T_c = 298.15$ K, velocity of the mainstream flow $U_\infty = 12$ m/s, and initial jet and mainstream turbulence Tu = 10 %. The flow exit condition is set as pressure outlet $P_{out} = 101325$ Pa. For all simulation cases, 2 blowing ratios M = 0.5 and M = 1 were considered. The blowing ratio is calculated as follows:

$$M = \frac{\rho_c U_c}{\rho_\infty U_\infty} \tag{5}$$

where, ρ_∞ and ρ_c are the mainstream flow and coolant jet densities , U_∞ and U_c are the mainstream flow and coolant jet velocities, respectively.

Table 2 Simulation parameter conditions.

Boundary conditions		**Physical parameters**	
U_∞ [m/s]	12	d [mm]	12.7
T_∞ [K]	331.15	p/d	3
T_c [K]	298.15	y/d	5
DR	1	α [°]	35

Results and discussion

In this research work, the adiabatic, lateral and area-averaged film cooling effectiveness results which are described by formulas (6), (7) and (8) respectively, were presented.

$$\eta = \frac{T_\infty - T}{T_\infty - T_c} \tag{6}$$

$$\bar{\eta} = \frac{1}{L}\int_L \eta dz \tag{7}$$

$$\bar{\bar{\eta}} = \frac{1}{A}\iint_A \eta dA \tag{8}$$

where L and A represent the spanwise dimension and cooled are, respectively.

For calculation method validation reason, lateral averaged cooling effectiveness results of the present work are compared with the experimental data of Nasir *et al.* [21] as presented in **Figure 4**. Maximum difference between the numerical solution and experimental data of 37 % was observed at x/d = 15 which means an effectiveness difference value of 0.02. In general, good agreement of numerical results of this study with the experimental measurements is obtained, which demonstrates the good accuracy of film cooling numerical prediction using ANSYS CFX code and SST turbulence model.

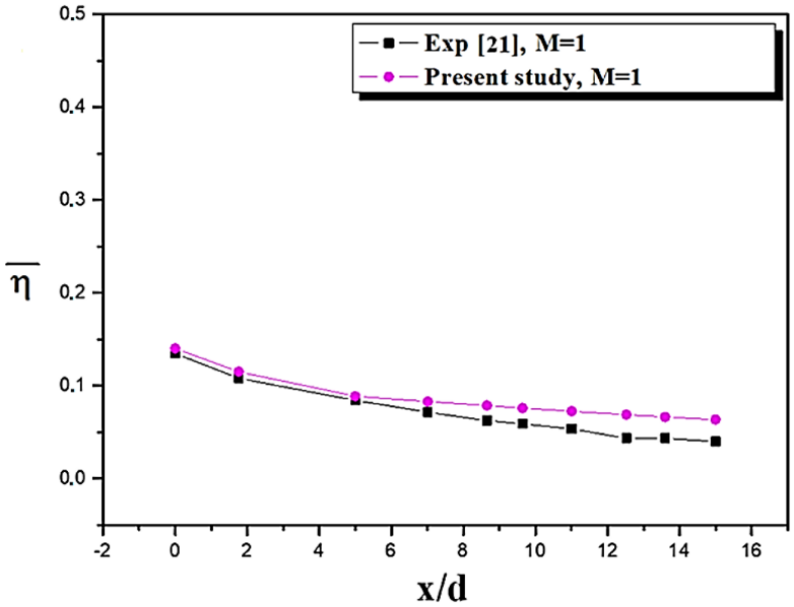

Figure 4 Laterally averaged adiabatic film cooling effectiveness.

The effects of crescent shaped block length (B = 0.5d, 1d and 1.5d) on centerline film cooling effectiveness for M = 0.5 is presented in **Figure 5**. We can clearly see that the centreline effectiveness increases by increasing the block length. The higher centreline effectiveness distribution is obtained for Model 6 (B = 1.5d, W = 2d).

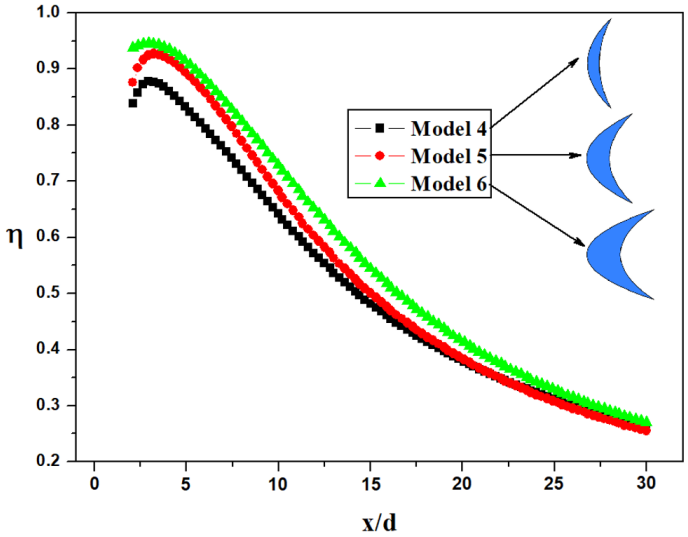

Figure 5 Centreline adiabatic film cooling effectiveness at various block lengths (B = 0.5d, 1d and 1.5d) and a constant block width W = 2d for M = 0.5.

Figure 6 presents the lateral film cooling effectiveness at plan x/d = 3 for different block widths (W = 1d, 2d and 3d) and a block length B = 0.5d. It is clear that the lateral adiabatic cooling effectiveness in the region (−0.5 < z/d < 0.5) for Model 1 and 4 is significantly higher than that in the Model 7. However, in the presence of Model 7 (W = 3d), the cooling film spreads very well in the lateral direction compared to other cases.

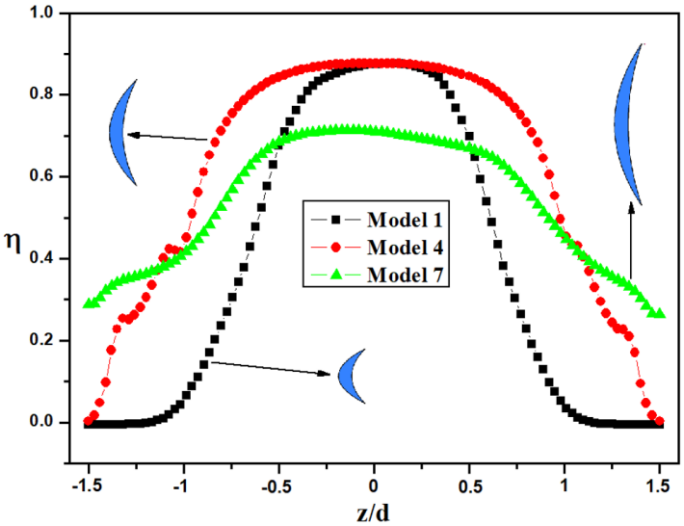

Figure 6 Lateral adiabatic film cooling effectiveness at various block widths (W = 1d, 2d and 3d) and a constant block length B = 0.5d for M = 0.5.

Area average effectiveness at various crescent shaped block configurations for M = 1 is illustrated in the **Figure 7**. For block models widths W = 1d and W = 2d (models 1-6), the area average effectiveness decreases slightly with increasing the length (B) of the crescent shaped block. However, for W = 3d (models 7 - 9), higher area average effectiveness values are observed at B = 1d compared to other block configurations. For all cases, the lowest values of area average effectiveness were obtained at low crescent shaped block width W = 1d (models 1 - 3). This can be explained by the poor coverage expansion of the cooling film in lateral direction.

Figure 8 shows the effectiveness distributions contours for all cases at M = 0.5. For models with different block lengths (models 1 - 3, 4 - 6, 7 - 9), it is quite clear that increasing the block length provokes a slight increase of effectiveness along the streamwise direction. Considerable cooling coverage expansion is observed in models 7 - 9 (W = 3d) compared to other models which confirms the positive effects of

higher block width values on the coverage of film cooling. The optimum distribution of film cooling effectiveness is obtained using the Model 9.

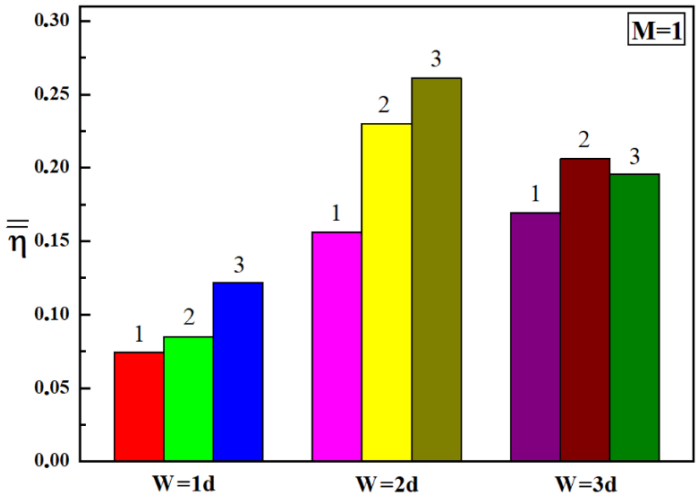

Figure 7 Cooling effectiveness averaged over the area of the cooled surface for M = 1 and different shaped block cases: B = 0.5d (1), 1d (2), and 1.5d (3).

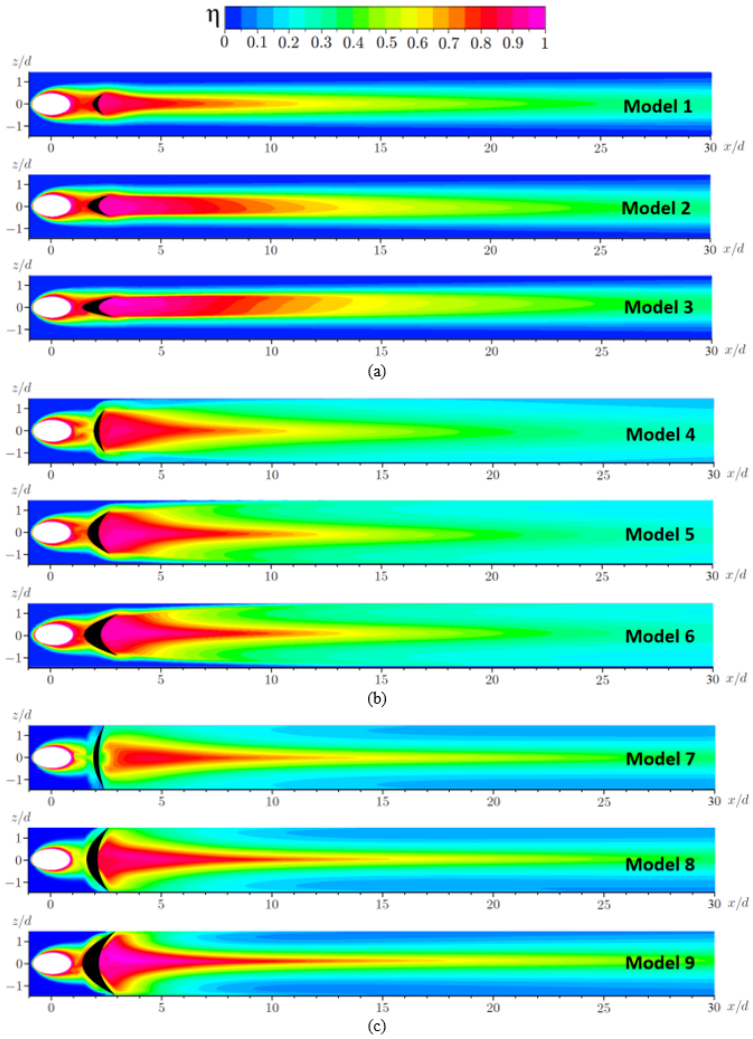

Figure 8 Contours of film cooling effectiveness for all cases at M = 0.5: W = 1d (a), W = 2d (b), W = 3d (c).

Figure 9 illustrates the velocity field overlaid with the dimensionless temperature (T/T_∞) to better show the impact of several crescent shaped block models on the contra-rotating vortex pair (CRVP). For all investigated models, the contours are shown on lateral plane x/d = 3 and at low blowing ratio M = 0.5. For models 1 - 3 which have the lower length value (B = 0.5d), a contra-rotating vortex pair is clearly appeared. By increasing the width of crescent shaped block (models 4 - 6), the shape and intensity of the CRVP increases. For high width models (7 - 9), the CRVP configuration changes by creating 2 other vortices at the lateral ends of the plate. These CRVP pulls the hot flow closer to the cooled wall and pushes the coolant away which decreases the film cooling effectiveness. Increasing the block length shows a slight increase in CRVP intensity for all models.

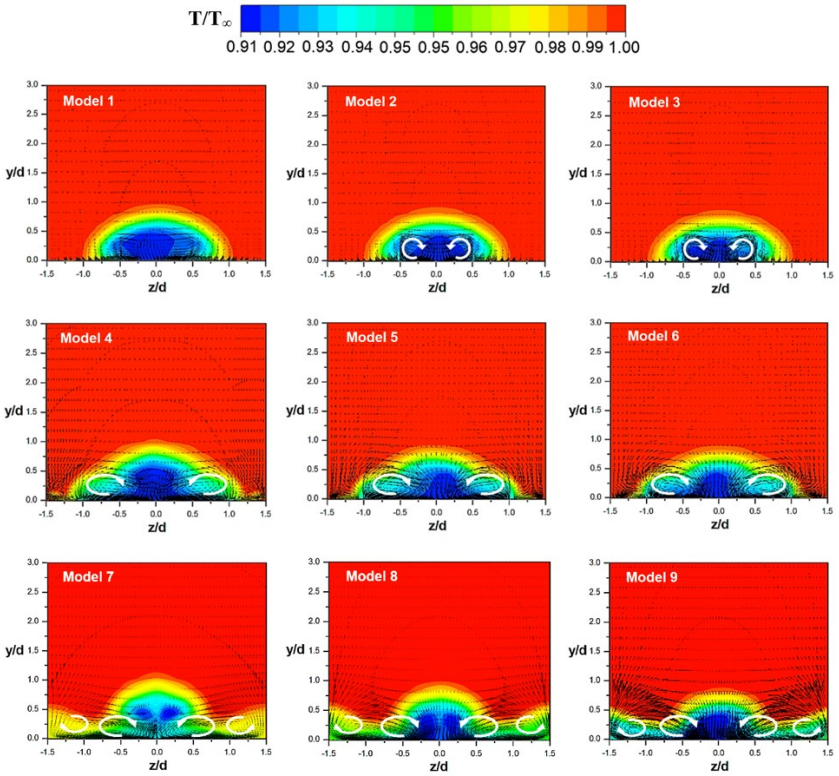

Figure 9 Velocity field distributions on the y-z plane at x/d = 3 for M = 0.5.

Conclusions

In the present study, the effects of crescent shaped block length and width on film cooling performance have been studied numerically. Nine different block models are considered by changing the block width (W = 1d, 2d, 3d) and block length (B = 0.5d, 1d, 1.5d). ANSYS CFX CFD code has been employed to conduct the 3-dimensional film cooling numerical simulations. The results of film cooling performance were illustrated for 2 blowing ratios (M = 0.5, 1). A good agreement with precedent experimental data has been obtained.

Based on the results, the film cooling performance is considerably influenced by the variation of block width compared to block length. Wider blocks promote a very good coverage of cooling film on the cooled surface. For M = 1, maximum area averaged effectiveness is obtained at model 6 (W = 2d, B = 1d). For all cases, higher values of effectiveness were obtained at model 9 (W = 3d, B = 1.5d). For all investigated models, the appearance of CRVP was observed. Increasing the bloc width increases the CRVP intensity and shape. However, block length variation has not a significant effect on CRVP shape. The maximum enhancement in overall film cooling effectiveness using the optimal configuration (model 6: W = 2d, B = 1.5d) is about 252 % achieved at a blowing ratio of M = 1. This percent is calculated as the difference between the overall film cooling effectiveness of model 6 (W = 2d, B = 1.5d) and model 1 (W = 1d, B = 0.5d) divided by that of model 1.

Acknowledgements

The corresponding author, Dr. Guelailia Ahmed, dedicates this paper to the memory of Dr. Boudjemai Abdelmadjid.

References

[1] HD Ammari and D Lampard. The effect of density ratio on the heat transfer coefficient from a film cooled flat plate. *ASME J. Turbomach.* 1990; **112**, 444-50.

[2] AK Sinha, DG Bogard and ME Crawford. Film-cooling effectiveness downstream of a single row of holes with variable density ratio. *ASME J. Turbomach.* 1991; **113**, 442-9.

[3] U Drost and A Bölcs. Investigation of detailed film cooling effectiveness and heat transfer distributions on a gas turbine airfoil. *ASME J. Turbomach.* 1999; **121**, 233-42.

[4] CL Liu, HR Zhu and ZW Zhang. Experimental investigation on the leading edge film cooling of cylindrical and laid-back holes with different hole pitches. *Int. J. Heat Mass Transfer*. 2012; **55**, 6832-45.

[5] A Guelailia, A Khorsi and MK Hamidou. Computation of leading edge film cooling from a console geometry (converging slot hole). *Thermophys. Aeromech.* 2016; **23**, 33-42.

[6] J Wang, K Tian and J Luo. Effect of hole configurations on film cooling performance. *Numer. Heat Tran. A Appl.* 2019; **75**, 725-38.

[7] N Cao, X Li and Z Wu. Effect of film hole geometry and blowing ratio on film cooling performance. *Appl. Ther. Eng.* 2020; **165**, 114578.

[8] K Tian, J Wang and C Zhanxiu. Effect of hole blockage configurations on film cooling in gas turbine components. *Chem. Eng. Trans*. 2017; **61**, 229-34.

[9] DL Schmidt and DG Bogard. Effects of free-stream turbulence and surface roughness on film cooling. *In*: Proceedings of the International Gas Turbine and Aeroengine Congress and Exhibition, Birmingham, UK. 1996.

[10] DL Schmidt, B Sen and DG Bogard. Effects of surface roughness on film cooling. *In*: Proceedings of the International Gas Turbine and Aeroengine Congress and Exhibition, Birmingham, UK. 1996.

[11] RJ Goldstein, ERG Eckert and HD Chiang. Effect of surface roughness on film cooling performance. *ASME J. Eng. Gas Turbines Power*. 1985; **107**, 111-6.

[12] A Guelailia, A Khorsi and SA Slimane. Numerical investigation on the effect of deposits height and position on the film cooling efficiency. *J. Appl. Mech. Tech. Phys.* 2020; **61**, 70-7.

[13] CHN Yuen and RF Martinez-Botas. Film cooling characteristics of a single round hole at various streamwise angles in a crossflow: Part I effectiveness. *Int. J. Heat Mass Transfer*. 2003; **46**, 221-35.

[14] CHN Yuen and RF Martinez-Botas. Film cooling characteristics of a single round hole at various streamwise angles in a crossflow: Part II heat transfer coefficients. *Int. J. Heat Mass Transfer*. 2003; **46**, 237-49.

[15] A Guelailia, A Khorsi, SA Slimane, H Blala, A Slimane, H Salem and A Bouferrouk. Effect of lid height and blowing ratio on film cooling effectiveness of a novel lidded hole configuration. *J. Proc. Mech. Eng.* 2022; **236**, 2599-607.

[16] A Guelailia, A Khorsi and AM Boudjemai. Thermal protection of rocket nozzle by using film cooling technology-effect of lateral curvature. *Int. J. Heat Tech*. 2018; **36**, 1070-4.

[17] A Guelailia, A Khorsi and SA Slimane. CFD analysis of film cooling applied on longitudinally curved walls. *Thermophys. Aeromech.* 2022; **3**, 751-9.

[18] AL Kumar, J Pisharady and SR Shine. Effect of injector configuration in rocket nozzle film cooling. *Heat Mass Transfer*. 2015; **52**, 727-39.

[19] A Khorsi, A Guelailia and MK Hamidou. Improvement of film cooling effectiveness with a small downstream block body. *J. Appl. Mech. Tech. Phys.* 2016; **57**, 666-71.

[20] A Guelailia, A Khorsi, SA Slimane, AM Boudjemai, A Smahat and P Kumar. CFD analysis of film cooling applied on longitudinally curved walls. *Thermophys. Aeromech.* 2022; **29**,751.

[21] H Nasir, SV Ekkad and S Acharya. Effect of compound angle injection on flat surface film cooling with large streamwise injection angle. *Exp. Ther. Fluid Sci*. 2001; **25**, 23-9.

[22] FR Menter. Two-equation eddy-viscosity turbulence models for engineering applications. *AIAA J*. 1991; **32**, 1598-605.